ACS Catalysis

Research Article

pubs.acs.org/acscatalysis

Impacts of Organic Stabilizers on Catalysis of Au Nanoparticles from Colloidal Preparation

Ru-Yi Zhong, Ke-Qiang Sun, Yong-Chun Hong, and Bo-Qing Xu*

Innovative Catalysis Program, Key Lab of Organic Optoelectronics & Molecular Engineering, Department of Chemistry, Tsinghua University, Beijing 100084, China

Supporting Information

ABSTRACT: Metal nanoparticles (NPs) from colloidal synthesis are advantageous in fundamental catalysis research because of their precisely controlled size and morphology but unfortunately are usually contaminated with residues from the organic stabilizer essentially required in the synthesis. These residues could modify the surface property and disturb the catalysis intrinsic to "clean" NPs. Herein, polyvinylpyrrolidone (PVP)-stabilized Au NPs (4.7 ± 1.0 nm) from colloidal synthesis were immobilized on SiO_2 support and subjected to ultraviolet-ozone (UVO) treatment to remove the residues. Hydrogenation reactions of *p*-chloronitrobenzene (*p*-CNB) and cinnamaldehyde (CAL) were conducted to probe consequences of the stabilizer removal on the catalytic properties of Au NPs. Measurements by FTIR and XPS revealed a controlled removal and degradation of PVP according to the UVO-treatment duration. Careful HRTEM analysis disclosed that both the size and morphology of Au NPs remained unchanged after the UVO-treatment. Residual PVP significantly improved the activity of Au NPs for *p*-CNB hydrogenation but lowered the activity for CAL hydrogenation. Continued selectivity changes of CAL hydrogenation to favor the reaction at the C═C bond were observed on increasing the removal degree of the residues. The UVO-cleaned Au NPs were also "restabilized" with PVP and other stabilizers by adsorption in aqueous solution. Comparison of the catalytic properties of these Au NPs involving different stabilizers with those of the UVO-cleaned ones enabled a comprehension of the stabilizer impacts on the hydrogenation catalysis of Au NPs.

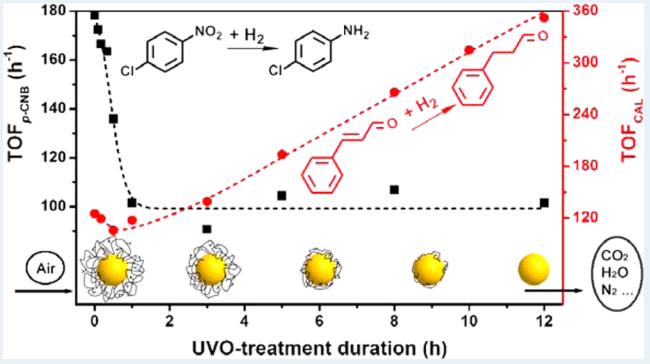

KEYWORDS: *catalysis by gold, metal colloids, selective hydrogenation, stabilizer effect, ultraviolet-ozone, chloronitrobenzene, cinnamaldehyde*

1. INTRODUCTION

Au nanoparticles (NPs) have attracted extensive interest since the late 1980s for their unique size-dependent catalytic properties and versatile applications in chemical syntheses, energy conversion, and environmental protection.[1] Investigations on the catalytic properties of Au NPs with narrow size distribution[2,3] and/or specific facets[4] would gain insight on the fundamental nature of active sites. By varying the type[5,6] or dosage[3,7] of stabilizers in colloidal synthesis, the metal particle size and/or morphology can be precisely tailored. Typical stabilizers used in controlled synthesis of Au NPs include small molecules such as citrate (Citr)[5,8] and cetyltrimethylammonium bromide (CTAB),[4] or polymers such as polyvinylpyrrolidone (PVP)[2,3,5,7,9] and poly(vinyl alcohol) (PVA).[3,5,10] Among the various stabilizers, PVP has received a broad attention for its chemical stability, nontoxicity, and excellent solubility.[11]

Au NPs from colloidal synthesis can be immobilized onto a wide range of supports, such as SiO_2,[10,12] Al_2O_3,[12,13] and carbon.[5,12] This two-step strategy (colloidal synthesis and then immobilization) allows for a finer control of the Au size and morphology compared to conventional preparation approaches like impregnation or deposition-precipitation.[3] However, a part of the organic stabilizer would remain as surface residue in the final catalysts and impact the property and catalysis of their stabilized Au NPs,[3,5,13−17] which could significantly disturb our study on the true structure−property relationship intrinsic to "clean" Au NPs. Possible effects of the stabilizer-residue would include steric blocking of the catalytic sites,[3,13−17] modifying the electronic state[5,18] and interaction[13] of Au NPs with the support, and so forth. However, most work regarding the catalysis of Au NPs from colloidal synthesis has focused on the size and/or morphology feature, the role of stabilizers has been seldom discussed.[2,4,5,7] It remains unclear how the stabilizer residues would disturb the catalysis of Au NPs at the molecular scale.

Several protocols have been proposed in earlier investigations of the stabilizer effects on catalysis by metal NPs. The

Received: August 8, 2014
Revised: September 24, 2014
Published: September 25, 2014

seemingly convenient one is to compare the catalytic activities of metal NPs synthesized using different stabilizers.[3,5,13,19] Because the size and morphology of the resulting metal NPs may differ significantly, it is often difficult to isolate and assess the stabilizer effects on the catalytic performance. Another approach is via postsynthesis modification of Au NPs,[13,20,21] like adding stabilizers to supported Au NPs from deposition-precipitation,[13] exchanging CTAB-stabilized[20] or Citr-stabilized[21] Au NPs with other stabilizers. The introduction of a stabilizer to supported Au NPs from "stabilizer-free" preparations could lead to unwanted modification to the support surface,[13] whereas the stabilizer-exchange approach would have difficulties in ensuring similar coverage and complete exchange for different stabilizers.[22,23]

A straightforward approach would be to compare the catalytic performance of Au NPs before and after removal of the surface stabilizers.[14−17] Many attempts were made to eliminate stabilizer-residue from the metal NPs but usually with little attention paid to avoiding undesirable side effects. The commonly used high-temperature (oxidation) treatment could compromise the size and morphology of the metal NPs,[14,15,24] the metal−support interaction,[14,15] and perhaps lead to secondary residues poisonous to the catalytic sites.[25] Wet chemical methods like washing with different solvents[16,21−24] or oxidation by $KMnO_4$[17] could only partly remove the stabilizer residues, induce aggregation of the metal NPs, and even cause further contamination from the reagents.[16,17,24] Recently, ultraviolet-ozone treatment (UVO-treatment) that combines excitation by UV light with the oxidation by ozone[26] was applied to eliminate the PVP stabilizer from PVP-stabilized Pt[27] and Pd[28] NPs under ambient conditions. The sizes and morphology of the noble metal NPs almost showed no change before and after UVO-treatment.[27,28] Though more or less passivation of the NP surface by chemisorbed oxygen was detected during the UVO-treatment,[27,28] a follow up mild reduction with hydrogen could eliminate such passivation,[28] making UVO-treatment a promising technology for the removal of organic stabilizers from immobilized metal colloids. However, it remains unknown if the same technology could be applicable for quantitative removal of organic stabilizers from the less stable Au NPs. Also, the cleanness or removal degree of the UVO-treated metal NPs was usually not comprehensively probed with surface-sensitive techniques (e.g., XPS).

The UVO-treatment technology is used herein to systematically vary the removal degree of PVP and its derived secondary residues on nearly monodisperse PVP-stabilized Au NPs. Comprehensive characterizations using transmission electron microscopy (TEM), Fourier-transform infrared spectroscopy (FTIR), and X-ray photoelectron spectroscopy (XPS) are conducted to ascertain that both the size and morphology of Au NPs remain unchanged after the UVO-treatment. The UVO-treated samples are then used to assess impacts of the stabilizer on the catalysis by Au NPs using hydrogenation of *p*-chloronitrobenzene (*p*-CNB) and cinnamaldehyde (CAL) as the probe reactions.[21] SiO_2 is used to immobilize the Au NPs because it is a widely accepted neutral support material for metal NP catalyst.[29] Previously, Au NPs were found highly selective for *p*-chloroaniline (*p*-CAN) production in *p*-CNB hydrogenation,[30−32] and showed an interesting structure sensitivity in CAL hydrogenation.[33−36] "Restabilization" of the UVO-cleaned Au NPs with different stabilizers (i.e., PVP, PVA, CTAB, and Citr) is also done to prepare samples containing the same Au NPs but involving different stabilizers, whose catalytic consequences are assessed by comparing the catalytic properties of these Au NPs with those of the UVO-treated ones. The data entitle a comprehensive discussion on the nature of active Au sites for the hydrogenation catalysis.

2. EXPERIMENTAL SECTION

2.1. Preparation and Immobilization of Au NPs Stabilized by PVP and Citr. The PVP-stabilized Au NPs of 4.7 ± 1.0 nm (Au-PVP) were synthesized via a seed-mediated method, as detailed in our earlier publications.[5,9,37] Immobilization of the Au-PVP NPs on SiO_2 powders (Degussa, AEROSIL 90, SBET = 90 $m^2 \cdot g^{-1}$) was conducted using the procedure reported previously.[9,21,36] Unless otherwise specified, the content of Au was fixed at 1.00 ± 0.05 wt%, as confirmed by ICP-AES analysis. The resultant Au-PVP/SiO_2 powders were dried in air at 110 °C and were stored in a refrigerator for later use.

2.2. UVO-Treatment. UVO-treatment of Au-PVP/SiO_2 was carried out using a U-shape low pressure mercury lamp (BIOZONE, 10-11100, 20 w) at ambient temperature in flowing air (70 $mL \cdot min^{-1}$), for varying periods (0.1 to 12 h), in order to control the removal of PVP residues. The lamp emits mainly ultraviolet radiations at 184.9 and 253.7 nm; the former can generate highly oxidative ozone and atomic oxygen from ambient oxygen (air), and the latter can excite organics and promote their oxidation to H_2O, CO_2, and N_2.[26] The lamp was mounted in a tubular glass reactor (i.d., 60 mm; length, 500 mm), as shown in Figure S1 (Supporting Information). The reactor was wrapped with an aluminum foil to prevent leak of UV light. The sample (Au-PVP/SiO_2) powders were dispersed at a thickness of ca. 0.6 mm on a glass slide placed 6 mm apart from the lamp surface.[27,28] The resulting sample was coded as Au-PVP/SiO_2-*t*UVO according to the UVO-treatment duration *t* in hour.

2.3. Restabilization of UVO-Cleaned Au-PVP/SiO_2 Samples. UVO-treatment for 12 h was found to be a suffcient duration to completely clean the Au-PVP/SiO_2 sample from organic residues. Restabilization with PVP of this UVO-cleaned sample (Au-PVP/SiO_2-12UVO) led to RePVP(Au-PVP/SiO_2-12UVO), which was obtained by immersing Au-PVP/SiO_2-12UVO in an aqueous solution of PVP (molar PVP-monomer/Au = 100) for 2 h under stirring, followed by separation of the solids by filtration and then drying without washing at 110 °C. A sample coded as RePVP(Au-PVP/SiO_2-12UVO)-W was also made by adding an extensive washing step (with deionized water) prior to the drying step. Similar restabilization with PVP of the Au-PVP/SiO_2-*t*UVO samples (*t* = 1 and 3 h) produced the RePVP(Au-PVP/SiO_2-*t*UVO samples, respectively. Alternatively, a restabilization with PVA, CTAB or Citr of Au-PVP/SiO_2-12UVO produced the RePVA(Au-PVP/SiO_2-12UVO), ReCTAB(Au-PVP/SiO_2-12UVO), or ReCitr(Au-PVP/SiO_2-12UVO) sample.

2.4. Characterization Methods. TEM measurements were conducted on a Tecnai G2 F20 U-Twin microscope at 200 kV. At least 300 particles were randomly measured to determine the mean diameter of Au NPs, using the equation $d = \Sigma(n_i d_i)/\Sigma n_i$, where n_i is the number of particles with a diameter of d_i. High-resolution TEM (HRTEM) images were obtained on a Tecnai G2 F20 S-Twin microscope at 300 kV. Further details of the TEM/HRTEM measurements were given previously.[37]

FTIR studies were made on a PerkinElmer 2000 system. For rigorous comparison of the intensity of the absorption bands,

dx.doi.org/10.1021/cs501161c | ACS Catal. 2014, 4, 3982−3993

the sample powders were ground with 12-fold KBr powders (by weight) and then pressed into a wafer of 36.0 mg (diameter 13 mm) for the measurement. The spectra were recorded at a resolution of 4 cm^{-1} from 4000 to 500 cm^{-1}, accumulating 10 scans per spectrum.

XPS measurements were performed on a PHI 5300 ESCA1610 SAM spectrometer equipped with a Mg Kα radiation (1253.6 eV); the precision in measuring the binding energy (BE) was within ±0.1 eV. The spectra for N 1s and Au 4f were scanned 60−200 times to improve the signal-to-noise ratio. The BE for C 1s in adventitious contaminants on "pure" SiO_2 support was set at 284.8 eV for charge correction, and then used to calibrate the BEs for the other elements (Au 4f, N 1s, Si 2p and O 1s). The atomic fraction data for different elements (Au, N, O, Si, and C) at the sample surface were obtained according to their XPS peak areas after subtraction from Shirley-type backgrounds, using empirical cross section factors. The C 1s and Au 4f spectra were analyzed by curve-fitting using Gaussian-type peaks. Deconvolution of the Au 4f spectra into Au $4f_{5/2}$ and $4f_{7/2}$ doublets was done with a BE separation of 3.7 eV and an area ratio of 0.75.

2.5. Catalytic Hydrogenation Reactions of *p*-CNB and CAL. The hydrogenation reactions were performed in a 25 mL stainless steel autoclave under magnetic stirring (900 rpm).[27,33] No mass-transfer (diffusion) limitation during the reactions was confirmed by Madon−Boudart tests[10,38] of Au-PVP/SiO_2 samples with various Au loadings (Figure S2). Blank tests with bare SiO_2 and PVP-loaded SiO_2 but without Au NPs detected no reaction of either *p*-CNB or CAL.

3. RESULTS AND DISCUSSION

3.1. Removal of PVP Residues by UVO-Treatment. *3.1.1. FTIR and XPS Studies.* Figure 1A shows the IR spectra of

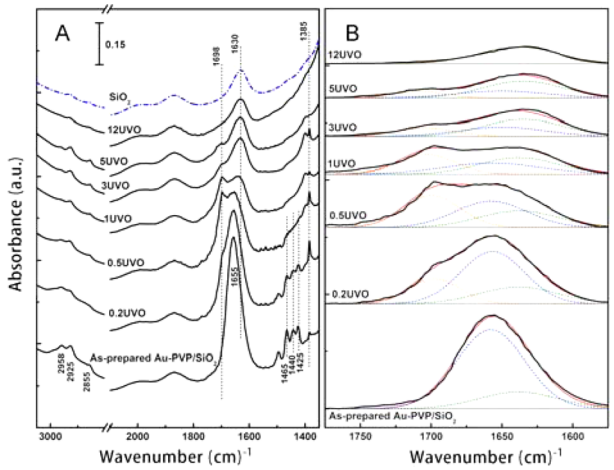

Figure 1. FTIR spectra for Au-PVP/SiO_2 samples of different UVO-treatment durations; the up-most curve (blue) shows the spectrum for the "pure" SiO_2 support (A). Deconvolution of the overlapped bands in the range of 1550−1750 cm^{-1} (B).

Au-PVP/SiO_2 with different UVO-treatment durations. The absorption bands and their assignments are summarized in Table S1. The bands in the region of 3000−2800 cm^{-1} were CH_2 stretching vibrations in the hydrocarbon backbone and the pyrrolidone rings, and the ones in 1500−1400 cm^{-1} were C−N stretching and C−H scissoring vibrations.[39,40] The 1655 cm^{-1} band was mainly associated with C═O stretching vibration. Overall, these PVP-associated IR bands became less intensified on increasing the duration, indicating a removal and/or degradation of PVP-residue from the sample.

A new band at 1698 cm^{-1} appeared shortly after exposure to the UVO-treatment ($t \leq 0.2$ h), accompanied by a distinct intensification of the 1385 cm^{-1} band. These two bands can be ascribed to the C═O stretching (1698 cm^{-1}) and C−O−H in-plane bending (1385 cm^{-1}) modes of carboxylic groups.[40] These two bands became most intensified at t = 0.5 h and then decreased gradually on further t increasing, indicating that the PVP-residue was first oxidized to intermediates featuring the carboxylic groups. When t was extended to 12 h, the spectrum became essentially the same as that of SiO_2, suggesting a complete removal of PVP and its derived surface residues; the remaining band at 1630 cm^{-1} signified the H−O−H bending vibration of adsorbed H_2O on SiO_2, whereas the ones at 2009 and 1870 cm^{-1} are the overtones of Si−O stretching vibrations.[41,42]

Figure 1B presents the band deconvolution curves in the region of 1550−1750 cm^{-1}, involving the C═O stretching and H−O−H bending vibrations. Although the band intensities (i.e., peak area) could measure the concentration of their associated species because the spectra were recorded on carefully prepared wafers with consistently weighted composition and mass (as indicated by the invariant overtones of the Si−O stretching modes in Figure 1A), the invariant intensity of the 1630 cm^{-1} band (bending vibration of adsorbed water on SiO_2) from the deconvolution was taken as a reference to accurately quantify the intensities of the two C═O bands arising, respectively, from the carboxylic (1698 cm^{-1}) and carbonylic (1655 cm^{-1}) groups, which are shown as a function of t in Figure 2. Clearly, the PVP-specific carbonylic groups (1655 cm^{-1}) decreased monotonically with t, demonstrating a gradual and continuous degradation of PVP-residue during the treatment.

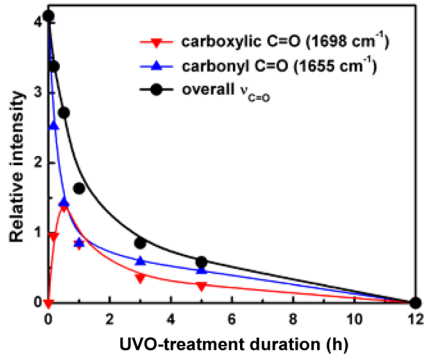

Figure 2. Intensities of the IR bands for carboxylic (1698 cm^{-1}) and carbonyl (1655 cm^{-1}) C═O stretching vibrations, in relation to that for the H−O−H bending vibration (1630 cm^{-1}) for adsorbed H_2O on the SiO_2 support.

The effect of UVO-treatment on the Au-PVP/SiO_2 sample was also characterized with XPS; the results are given in Figure 3 and Table S2. The Au $4f_{7/2}$ and $4f_{5/2}$ doublets were observed at 83.1 and 86.9 eV for the as-prepared Au-PVP/SiO_2, which were 0.9 eV lower than those for metallic Au reference (84.0 and 87.7 eV). This is indicative of electron transfer from PVP to Au, in agreement with earlier reports that as-synthesized PVP-stabilized Au NPs were negatively charged.[2,5,18,43] Apparently, the negative charge on these Au NPs came from

dx.doi.org/10.1021/cs501161c | ACS Catal. 2014, 4, 3982−3993

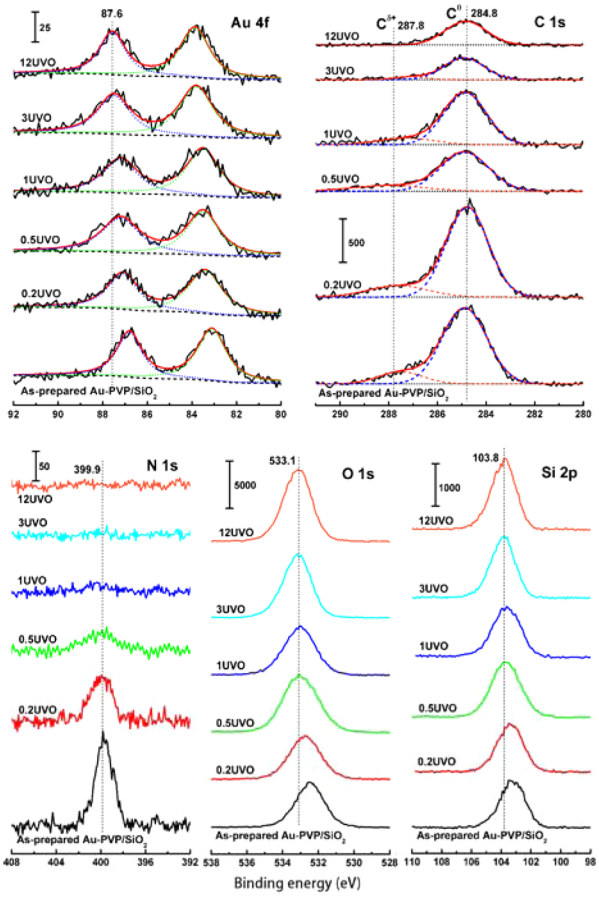

Figure 3. XPS spectra of Au 4f, C 1s, N 1s, O 1s, and Si 2p for Au-PVP/SiO_2 samples of different UVO-treatment durations.

electron donation from the oxygen atoms in the C═O groups of PVP molecules because the XPS signal for N 1s (399.9 eV) appeared at the same position as in pure PVP.[43] The BEs of Au 4f increased gradually upon the UVO-treatment and became equal to those for the reference Au when the UVO-treatment was continued for longer than ca. 3 h.

The changes of the XPS signals for C 1s and N 1s, also shown in Figure 3, demonstrate a simultaneous removal of C- and N-containing species during the UVO-treatment. The C 1s signal consisted of two components with BEs at 284.8 and 287.8 eV, which can be assigned to the C^0 atoms in the aliphatic parts and $C^{\delta+}$ atoms bound to the O and N atoms in the residues, respectively. The ratio $C^{\delta+}/C^0$ increased with the UVO-treatment duration up to t = 0.5 h and then kept on decreasing with t increasing (Table S2), which coincides well with the intensity change of the C═O stretching band (1698 cm^{-1}) (Figures 1B and 2). These data disclose the degradation of PVP-residue by photochemical oxidation into surface intermediates involving carboxylic groups, whose further oxidation would lead to volatile products like CO_2, H_2O and etc. The small C 1s signal at 284.8 eV on the Au-PVP/SiO_2-12UVO sample was arisen from adventitious hydrocarbon contaminants during the sample storage and preparation for XPS measurement.

As shown in the last two columns of Figure 3, increasing the UVO-treatment duration also resulted in shifts to higher binding energies (BEs) of the O 1s (from 532.5 to 533.1 eV) and Si 2p (from 103.3 to 103.8 eV) electrons. Their lower BEs in the as-prepared Au-PVP/SiO_2 were probably due to H-bonding between the SiO_2-based silanols and the carbonyl-based oxygen atoms in PVP-residue.[44] The BEs for O 1s and Si 2p increased to their "normal" positions for "pure" SiO_2 at $t \geq 1$ h, though their intensities generally increased until t = 12 h (Figure 3).

A reference PVP-SiO_2 sample was also prepared by PVP immobilization (adsorption) from an aqueous solution containing the same amount of PVP but without any Au NPs. Its IR spectra on exposure to the UVO-treatment are shown as Figure S3. Though the overall features of the spectra were similar to their Au-PVP/SiO_2 counterparts, the significantly less intensified signal for the carboxylic groups on PVP-SiO_2-1UVO than on Au-PVP/SiO_2-1UVO would indicate that the carboxylic groups in the intermediate associated with the Au NPs were more stable than those on the support (SiO_2) surface. This would explain why the XPS BEs for Au did not, but those for Si and O almost returned to their normal positions when the UVO-treatment duration was t = 1 h (Figure 3).

Therefore, our IR and XPS data are consistent in revealing a fast degradation and removal of the PVP stabilizer and its derived residues during the first hour of the UVO-treatment. Both sets of data also demonstrate a complete removal of the residual organics from both the Au NPs and their supporting SiO_2 by conducting the UVO-treatment for 12 h.

3.1.2. Sizes and Morphologies of Au NPs before and after the UVO-Treatment. Figure 4 shows the representative TEM

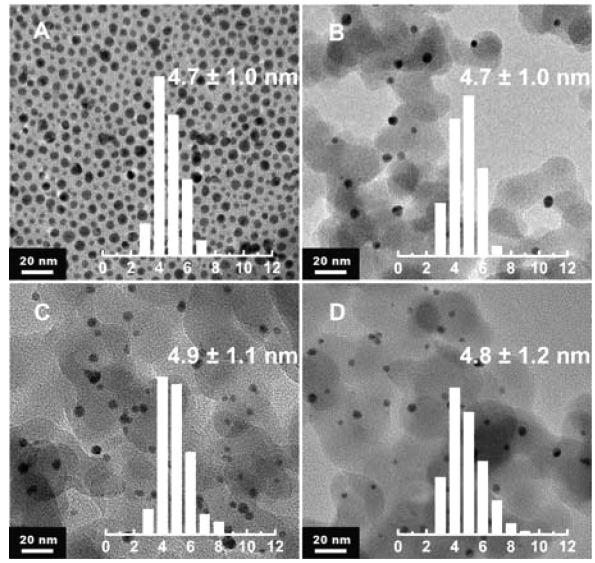

Figure 4. Representative TEM images for Au-PVP (A), Au-PVP/SiO_2 (B), Au-PVP/SiO_2-1UVO (C), and Au-PVP/SiO_2-12UVO (D).

images of Au-PVP, Au-PVP/SiO_2, Au-PVP/SiO_2-1UVO, and Au-PVP/SiO_2-12UVO. The sizes and shapes of Au NPs in the as-prepared Au-PVP/SiO_2 without UVO-treatment (4.7 ± 1.0 nm, Figure 4B) were essentially indistinguishable from those in Au-PVP/SiO_2-1UVO (4.9 ± 1.1 nm, Figure 4C) and Au-PVP/SiO_2-12UVO (4.8 ± 1.2 nm, Figure 4D); they all resembled their colloidal precursor particles (Au-PVP) prior to immobilization (4.7 ± 1.0 nm, Figure 4A). These observations clearly indicate that the sizes and shapes of Au NPs were kept invariant throughout the UVO-treatment.

Au NPs in the as-prepared Au-PVP sample are a mixture of single crystalline (S) and 5-twinned particles, according to our

dx.doi.org/10.1021/cs501161c | ACS Catal. 2014, 4, 3982−3993

earlier particle structure analysis by HRTEM.[37] Figure 5 shows some representative HRTEM images for the Au NPs in Au-PVP/SiO_2-tUVO (t = 0, 1, and 12 h) samples; the multitwinned particles were identified in two shapes, decahedra (Dh) and icosahedra (Ih). The observation that Dh and Ih particles were slightly larger than the S ones agrees with our earlier study on the particle morphology of colloidal and carbon-immobilized Au NPs.[37] Clearly, the Au NPs after UVO-treatment (e.g., in Au-PVP/SiO_2-1UVO and Au-PVP/SiO_2-12UVO, Figure 5B,C) also remained as a mixture of S, Dh, and Ih particles. The particle-shape selectivity data from careful HRTEM measurements are listed in Table 1. The overall selectivity for 5-fold twinned particles was 85−89% (by number of particles) for every sample, independent of the UVO-treatment duration. These data demonstrate that not only the Au particle sizes but also their internal particle structures were kept unchanged during the UVO-treatment.

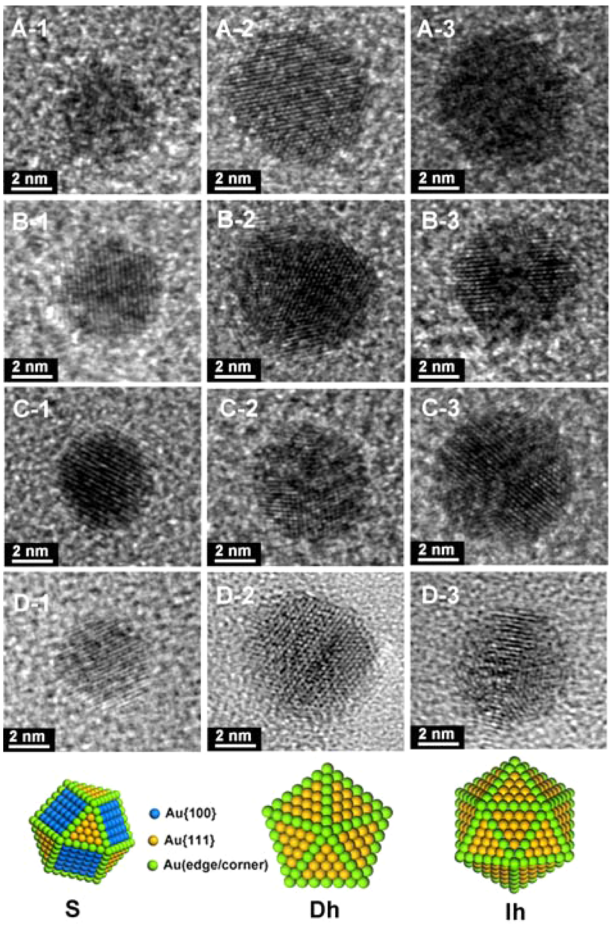

Figure 5. Representative HRTEM images of Au NPs for Au-PVP/SiO_2 (A), Au-PVP/SiO_2-1UVO (B), Au-PVP/SiO_2-12UVO (C), and RePVP(Au-PVP)/SiO_2-12h (D). Drawings in the bottoms show the model particle structures of the single (S), decahedral (Dh), and icosahedral (Ih) crystallites.

3.1.3. Degradation of PVP Residues by UVO-Treatment. The preceding data from FTIR, XPS, and TEM analyses are consistent in demonstrating that UVO-treatment can be developed as a method to clean the SiO_2-supported Au NPs (Au-PVP/SiO_2) from the stabilizer (PVP) without changing the sizes and shapes of the Au NPs. Moreover, the removal degree of the stabilizer could be controlled simply by changing the UVO-treatment duration.

Table 1. Particle Structure Selectivity for Au NPs in Au-PVP, Au-PVP/SiO_2, Au-PVP/SiO_2-1UVO, and Au-PVP/SiO_2-12UVO Samples

sample	Au size (nm)	(Ih + Dh)[a] (%)	S[b] (%)
Au-PVP	4.7 ± 1.0	87.2	12.8
Au-PVP/SiO_2	4.7 ± 1.0	86.6	13.4
Au-PVP/SiO_2-1UVO	4.9 ± 1.1	89.2	10.8
Au-PVP/SiO_2-12UVO	4.8 ± 1.2	87.4	12.6

[a]Ih and Dh denote, respectively, icosahedra and decanedra featuring 5-fold twinned particle structures. [b]S denotes single crystals.

For references, the as-prepared Au-PVP/SiO_2 was also treated by the reflux method described by Hutchings et al.[16] According to our FTIR evaluation of the C═O stretching absorption (Figure S4), the refluxing in water under stirring at 90 °C of Au-PVP/SiO_2 for 1 h (Au-PVP/SiO_2-R1) resulted in a removal of the PVP-residue by 25−30%, but an extension of the refluxing time to 4 h (Au-PVP/SiO_2-R4) did not lead to any further removal. Except their lower intensity, the overall feature of the IR spectra for these Au-PVP/SiO_2-R1 and -R4 samples appeared essentially the same as for the as-prepared Au-PVP/SiO_2, disclosing that the chemical state (structure) of the PVP stabilizer was kept intact during the reflux treatment. This may imply that the stabilizer removed during the reflux treatment was adsorbed mainly on the surface of SiO_2 (support). Accordingly, the sizes of Au NPs in Au-PVP/SiO_2-R4 were found by TEM in 4.9 ± 1.0 nm, showing no detectable size change during the reflux treatment.

Therefore, the present UVO-treatment method is advantageous to the reflux method[16] because it can lead to controlled removal of the residual stabilizer, up to a complete cleaning of the sample from the stabilizer. The control of the removal degree, while inducing essentially no change in the Au sizes and shapes, would also make the UVO-treatment method advantageous over the high-temperature calcination,[14,15,24] and chemical etching (e.g., using $KMnO_4$[17]) methods that were documented earlier for eliminating stabilizer-residue from immobilized metal NPs. It is expected that this UVO-treatment method could also be promising for removal of other stabilizers from supported metal NPs derived from colloidal synthesis.

The removal of PVP and its derived residues during the UVO-treatment is further assessed in Figure 6 according to the calibrated overall intensity of C═O (carbonylic and carboxylic) stretching vibrations (I_t/I_0) in the IR spectra (Figure 1) and the

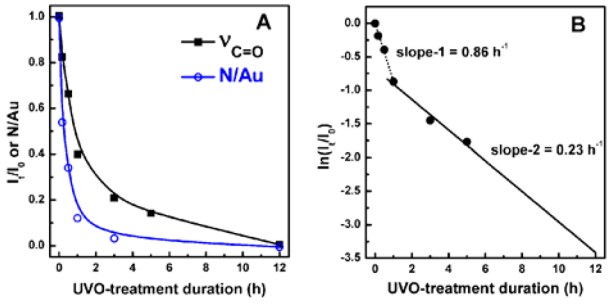

Figure 6. (A) Effects of UVO-treatment duration on the normalized C═O stretching vibration intensity (I_t/I_0) and XPS N/Au ratio. (B) Correlation between logarithm of I_t/I_0 and the UVO-treatment duration.

dx.doi.org/10.1021/cs501161c | ACS Catal. 2014, 4, 3982−3993

atomic N/Au ratio from XPS measurements (Figure 3), respectively. After UVO-treatment of 1 h, the N/Au ratio declined by ca. 88%, and the intensity of C═O declined by ca. 60%. The more rapid decline in the N/Au ratio might mean a faster elimination of N-containing species than those involving C═O groups.

To gain a kinetic image about the removal/degradation of the organic residues, the curve of I_t/I_0 versus t in Figure 6A was fitted in Figure 6B with a first-order removal kinetics, which gives a rate constant of 0.86 h^{-1} at $t \leq 1$ h and 0.23 h^{-1} at t = 1−12 h. Recalling that the most prominent changes to the surface residues during the first hour of the UVO-treatment were photochemical oxidations of the PVP-residue to surface species involving carboxylic groups and a preferred loss of nitrogen from the residues (Figures 1, 2, 3, and 6), it would be reasonable to speculate that in the initial stage of the UVO-treatment (t < 1 h) the PVP-residue experienced a fast photochemical degradation by simultaneously breaking the C−N bonds[49] and oxidizing the carbonyls in the pyrrolidone rings and (more or less) some terminal carbons to form the carboxylic-involving species. The significantly slower removal rate at t > 1 h could hint that these "secondary" surface species involving carboxylic groups could transform to some different residues more resistant to UVO-treatment. It is known that vinylcarbonates are cross-linkers in photopolymerization of *N*-vinylpyrrolidone under UV irradiations.[45] Thus, the slower removal rate at t > 1 h could be due to that such different residues were somehow cross-linked, as the surface species involving carboxylic groups can easily lead to formation of vinyl carbonates at the surface.

3.2. "Restabilization" of Au NPs with Different Stabilizers. The IR spectra for RePVP(Au-PVP/SiO_2-*t*UVO) of t = 1, 3, and 12 h are compared in Figure 7A with those for

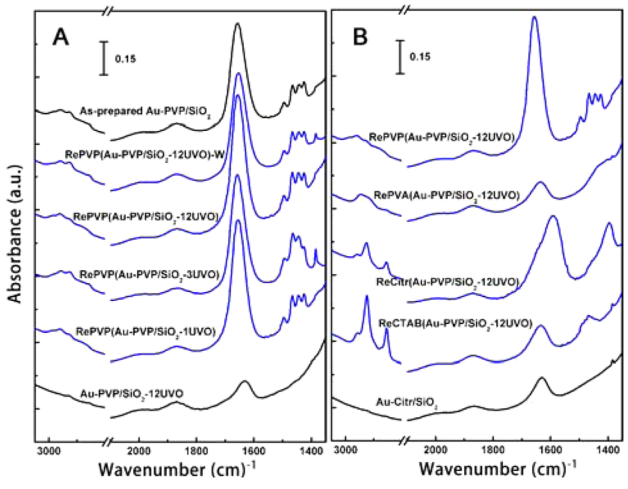

Figure 7. (A) Comparison by FTIR spectroscopy of RePVP(Au-PVP/SiO_2-*t*UVO) (t = 1, 3, and 12 h) and RePVP(Au-PVP/SiO_2-12UVO)-W samples with as-prepared Au-PVP/SiO_2 and Au-PVP/SiO_2-12UVO. (B) FTIR spectra of ReStabilizer (Au-PVP/SiO_2-12UVO) samples.

Au-PVP/SiO_2-12UVO and Au-PVP/SiO_2. The RePVP(Au-PVP/SiO_2-*t*UVO) samples were obtained by readsorption of PVP on Au-PVP/SiO_2-*t*UVO. Apparently, all the three RePVP(Au-PVP/SiO_2-*t*UVO) samples showed very similar spectra resembling to that for the as-prepared Au-PVP/SiO_2. Therefore, in spite of the differences in the UVO-treatment duration and thus the amount of the organic residues, the overall amounts of PVP stabilizer in the RePVP(Au-PVP/SiO_2-*t*UVO) samples appeared very similar. However, the spectrum for the washed sample (i.e., RePVP(Au-PVP/SiO_2-12UVO)-W) was ca. 20% less intensified than those for the unwashed RePVP(Au-PVP/SiO_2-*t*UVO) ones but was essentially the same as that for the as-prepared Au-PVP/SiO_2. These facts would indicate that the unwashed samples could involve some (ca. 20%) reversibly adsorbed PVP molecules that could become removed (via desorption) by extensive washing with deionized water.

Shown in Figure 7B are the IR spectra for RePVA(Au-PVP/SiO_2-12UVO), ReCTAB(Au-PVP/SiO_2-12UVO), and ReCitr-(Au-PVP/SiO_2-12UVO), which were obtained by "restabilization" of Au-PVP/SiO_2-12UVO with PVA, CTAB and Citr, respectively. The PVA stabilizer in RePVA(Au-PVP/SiO_2-12UVO) was characterized by the absorptions at 2925 and 2855 cm^{-1} (CH_2 stretching), 1460 cm^{-1} (broad, CH_2 scissoring), and 1385 cm^{-1} (C−O−H in-plane bending), though the signal characteristic of the stretching vibration for the polar C−O bond (ca. 1050 cm^{-1}) was overlapped by strong absorptions from the SiO_2 support. In the spectrum for ReCTAB(Au-PVP/SiO_2-12UVO), the absorptions at 2960, 2925, and 2855 cm^{-1} (C−H stretching), 1460 and 1385 cm^{-1} (C−H bending) denoted the alkyl chains of the CTAB stabilizer. The spectrum for ReCitr(Au-PVP/SiO_2-12UVO) gave two absorptions at 1580 (asymmetric) and 1400 cm^{-1} (symmetric) for R-COO^- vibrations; the absorptions in the region of 3000−2800 cm^{-1} were due to C−H stretching vibrations.

3.3. Catalytic Hydrogenation Study of Au NPs with and without Stabilizer Residues. Catalytic hydrogenation reactions of *p*-CNB[21,30,31] and CAL[10,21,33−35] were conducted respectively to assess the effects of PVP removal by UVO-treatment and the stabilizer nature on the catalytic property of Au NPs. The reactant conversion levels were controlled below 20% for rigorous comparison, and the catalytic activity was expressed by turnover frequency (TOF, h^{-1}) on surface Au atoms. The dispersion or exposed percentage of Au in each sample was taken as the reciprocal of their average Au particle size in nanometer. The reported TOF numbers (Figures 8 and 9, Tables 2 and 3) were obtained as the average rates from 3 to 5 replicate measurements; the relative errors were within 10%, mostly less than 6%.

3.3.1. Selective Hydrogenation of p-CNB. The hydrogenation of *p*-CNB produced *p*-CAN as the sole product according to GC analysis, as documented earlier on catalytic hydrogenation of nitroaromatics over Au NPs supported on ZrO_2,[30] TiO_2[31] and SiO_2.[32] Plotted in Figure 8 is the dependence on the UVO-treatment duration (t) of the Au activity according to *p*-CNB consumption ($TOF_{p\text{-CNB}}$) for the Au-PVP/SiO_2-*t*UVO catalysts. Apparently, $TOF_{p\text{-CNB}}$ declined rapidly with t up to 1 h (from 178 to 101 h^{-1}) and then remained in the vicinity of 100 h^{-1} on further t increasing. Considering the unaltered sizes and morphologies of the Au NPs during the UVO-treatment, these results are therefore strong indications that the presence of PVP[21] and its derived residues, especially those removed/reacted within the first hour of the UVO-treatment, were very beneficial to the Au catalysis for *p*-CNB hydrogenation.

The blue stars in Figure 8 report the Au $TOF_{p\text{-CNB}}$ data for RePVP(Au-PVP/SiO_2-*t*UVO) of t = 1, 3, and 12 h. In reference to the numbers for their Au-PVP/SiO_2-*t*UVO counterparts, the Au activity in RePVP(Au-PVP/SiO_2-1UVO) was slightly

dx.doi.org/10.1021/cs501161c | ACS Catal. 2014, 4, 3982−3993

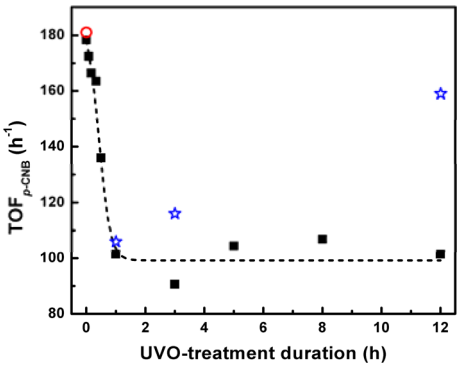

Figure 8. Effect of UVO-treatment duration on the Au activity by $TOF_{p\text{-CNB}}$ of Au-PVP/SiO_2 catalyst for *p*-CNB hydrogenation. The blue stars show the $TOF_{p\text{-CNB}}$ data for the Au in RePVP(Au-PVP/SiO_2-*t*UVO) (*t* = 1, 3, and 12 h); the red circle gives the TOF number for the Au-PVP/SiO_2-R1 catalyst.

higher, but those in RePVP(Au-PVP/SiO_2-3UVO) and RePVP(Au-PVP/SiO_2-12UVO) were distinctly higher (see also Table 2). Interestingly, the RePVP(Au-PVP/SiO_2-12UVO) became 94% active, and its washed counterpart RePVP(Au-PVP/SiO_2-12UVO)-W was already as active as the as-prepared Au-PVP/SiO_2, which further support the very beneficial effect of PVP to the Au catalysis for *p*-CNB hydrogenation.[21] The significant lower Au $TOF_{p\text{-CNB}}$ numbers for both RePVP(Au-PVP/SiO_2-1UVO) and RePVP(Au-PVP/SiO_2-3UVO) than that for RePVP(Au-PVP/SiO_2-12UVO) clearly demonstrate an "inhibiting" effect of the PVP-derived "secondary" residues involving carboxylic groups and/or vinyl carbonates, which could either prevent or shield the Au NPs from direct interaction or "restabilization" with the readsorbed PVP polymer. This indicates that not only the amount but also the nature of the organic residues impacted greatly the catalytic property of Au NPs.

The Au $TOF_{p\text{-CNB}}$ for ReCTAB(Au-PVP/SiO_2-12UVO) and ReCitr(Au-PVP/SiO_2-12UVO) appeared much lower, but that for RePVA(Au-PVP/SiO_2-12UVO) was even a little higher than that for RePVP(Au-PVP/SiO_2-12UVO) (Table 2). These differences reveal that the PVA stabilizer was at least as effective as PVP in enhancing the Au activity for *p*-CNB hydrogenation, but CTAB and Citr were detrimental to the Au catalysis. These results indicate that the nature of the stabilizer molecules impacts significantly the catalysis of Au NPs.

Table 2. Catalytic Data for Au NPs in Au/SiO_2 Samples Involving Different Stabilizers for *p*-CNB Hydrogenation Reaction[a]

catalyst	Au size (nm)	*p*-CNB conv. (%)	TOF[b] (h^{-1})
Au-PVP/SiO_2	4.7 ± 1.0	18.1	178
Au-PVP/SiO_2-12UVO	4.8 ± 1.2	10.3	101
RePVP(Au-PVP/SiO_2-12UVO)	4.8 ± 1.1	17.1	168
RePVP(Au-PVP/SiO_2-12UVO)-W		18.2	179
RePVA(Au-PVP/SiO_2-12UVO)		21.5	212
ReCitr(Au-PVP/SiO_2-12UVO)		0.4	4
ReCTAB(Au-PVP/SiO_2-12UVO)		2.0	20
Au-Citr/SiO_2[c]	11.1 ± 6.5	3.1	71
Au-PVP/SiO_2-R1		18.4	181
Au-PVP/SiO_2-R4	4.9 ± 1.0	18.4	181

[a]Rxn conditions: 50 mg catalyst, 2 mmol *p*-CNB, 5 mL toluene (solvent), P_{H_2} = 2 MPa, *p*-CNB/Au (molar) = 800, 150 °C, 4 h. [b]The TOF rates were based on the number of surface Au atoms, which were obtained from the average size of Au NPs assuming spherical shapes; the measurement errors were within 10% in repeated measurements or a deviation from these reported rates by ±5%. [c]Preparation details of this sample were described in ref 21.

3.3.2. Selective Hydrogenation of CAL. The hydrogenation of CAL could occur at either C═C or C═O bond, or both C═C and C═O bonds, leading to hydrocinnamaldehyde (HCAL) or cinnamyl alcohol (COL), or hydrocinnamyl alcohol (HCOL).[10,36] Figure 9 shows the activity and selectivity data of Au-PVP/SiO_2-*t*UVO for this reaction. The Au activity according to CAL consumption (TOF_{CAL}) decreased slightly when the UVO-treatment duration *t* was no longer than 1 h; however, the activity increased profoundly at *t* > 1 h and became 3-fold that for the as-prepared Au-PVP/SiO_2 (*t* = 0 h) at *t* = 12 h. These results indicate that the PVP stabilizer and its derived residues involving carboxylic groups (Figure 2) had a negative effect on the Au catalysis in the hydrogenation of CAL.

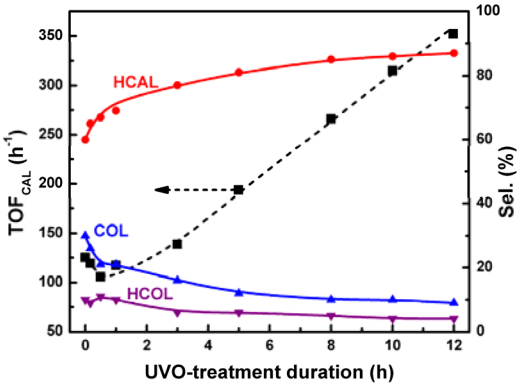

Figure 9. Effects of UVO-treatment duration on the Au activity by TOF_{CAL} and product selectivity of Au-PVP/SiO_2 catalyst for CAL hydrogenation.

The variation in *t* of the Au-PVP/SiO_2-*t*UVO catalyst also led to remarkable change in the product selectivity (Figure 9). The selectivity for HCAL increased from 60% at *t* = 0 h to 87% at *t* = 12 h at the expense of COL, which was reduced from 30% to 9%. Therefore, increasing the overall removal degree of the organic residues by increasing the UVO-treatment duration enhanced the selectivity for the hydrogenation at the C═C bond. Note that the selectivity change toward HCAL formation was most pronounced at $t \leq 1$ h.

Table 3 presents the results of CAL hydrogenation over the ReStabilizer(Au-PVP/SiO_2-12UVO) samples, together with those over Au-PVP/SiO_2 and Au-PVP/SiO_2-12UVO. The catalytic data for RePVP(Au-PVP/SiO_2-12UVO) were more or less close to those for the as-prepared Au-PVP/SiO_2, providing a further piece of support for the negative effects of PVP and its derived residues on Au catalysis for CAL hydrogenation.

The catalytic data for RePVA(Au-PVP/SiO_2-12UVO) were in the middle of those for Au-PVP/SiO_2 and Au-PVP/SiO_2-12UVO. Change of the ReStabilizer to CTAB (ReCTAB(Au-PVP/SiO_2-12UVO)) lowered the Au activity to the level for the as-prepared Au-PVP/SiO_2, but the selectivity for HCAL production was improved at the expense of COL. However, the use of Citr as the ReStabilizer (ReCitr(Au-PVP/SiO_2-

dx.doi.org/10.1021/cs501161c | ACS Catal. 2014, 4, 3982−3993

Table 3. Catalytic Data for Au NPs in Au/SiO_2 Catalysts Involving Different Stabilizers for the CAL Hydrogenation Reaction[a]

catalyst	CAL conv. (%)	product sel. (%) HCAL	COL	HCOL	TOF[b] (h^{-1})
Au-PVP/SiO_2	6.4	60	30	10	125
Au-PVP/SiO_2-12UVO	18.0	87	9	4	352
RePVP(Au-PVP/SiO_2-12UVO)	5.7	63	27	10	112
RePVP(Au-PVP/SiO_2-12UVO)-W	8.6	72	21	6	168
RePVA(Au-PVP/SiO_2-12UVO)	10.2	79	15	5	200
ReCitr(Au-PVP/SiO_2-12UVO)	1.3	14	52	35	25
ReCTAB(Au-PVP/SiO_2-12UVO)	6.7	74	15	11	131
Au-Citr/SiO_2[b]	5.8	72	20	7	263
Au-PVP/SiO_2-R1	6.1	59	33	8	119
Au-PVP/SiO_2-R4	5.7	65	29	6	112

[a]Rxn conditions: 50 mg catalyst, 4 mmol CAL, 5 mL xylene (solvent), P_{H_2} = 2.0 MPa, CAL/Au (molar) = 1600, 150 °C, 4 h. [b]See footnotes of Table 1.

12UVO)) made the Au NPs least active but distinctively more selective toward COL and HCOL.

3.4. Impacts of Stabilizers on Au Catalysis. A simple comprehension of the above characterization and catalytic hydrogenation results would point to a rich chemistry of the stabilizer effects on catalysis of Au NPs from colloidal synthesis. Not only the amount but also the nature of the stabilizer and its derived residues could impact significantly on the activity and/or selectivity of the Au catalyst.

Shown in the last two rows of Tables 2 and 3 are the catalytic data obtained over Au-PVP/SiO_2-R1 and -R4, which were essentially the same as or very close to those for the as-prepared Au-PVP/SiO_2 catalyst in the selective hydrogenation of both *p*-CNB and CAL. The indistinguishable catalytic performance of Au NPs in these three samples thus clearly demonstrates that the catalytic properties of the PVP-stabilized Au NPs were not affected during the reflux treatment in water, providing an indirect piece of evidence that the reflux treatment[16] could only remove PVP molecules being weakly adsorbed on SiO_2 surface but had no influence on those serving as the "real" stabilizer to the Au NPs. This strongly contrasted with the impacts of the UVO-treatment on the catalytic performance of the same Au-PVP/SiO_2 (Figures 8 and 9). Therefore, the removal and change of PVP and its derived residues due to the UVO-treatment would be responsible for the catalytic performance variations. In combination with the "intactness" of Au NPs to the UVO-treatment (Figures 4 and 5), it is therefore possible to address the impacts on Au catalysis of PVP and its derived residues without considering the size and morphology changes of Au NPs.

3.4.1. PVP Promotion of Au Catalysis in p-CNB Hydrogenation. The promotional role of PVP to the catalysis of Au NPs in the hydrogenation of *p*-CNB is well-supported by the distinctly higher $TOF_{p\text{-CNB}}$ numbers of the PVP-involving Au NPs in Au-PVP/SiO_2, RePVP(Au-PVP/SiO_2-12UVO) and RePVP(Au-PVP/SiO_2-12UVO)-W in comparison with that of the UVO-cleaned Au NPs in Au-PVP/SiO_2-12UVO (Table 2). To gain a deeper insight into this catalysis chemistry, we compare in Figure 10 the overall reaction kinetics over Au-PVP/SiO_2 (no UVO-treatment) and its UVO-cleaned counterpart Au-PVP/SiO_2-12UVO by showing the H_2 pressure drops as a function of the reaction time, using a calibrated Parr reactor. The pressure drops in the starting stage (<0.5 h) were coupled with unintended/unavoidable temperature fluctuation in calibrating the working pressure during the reactor heat up.

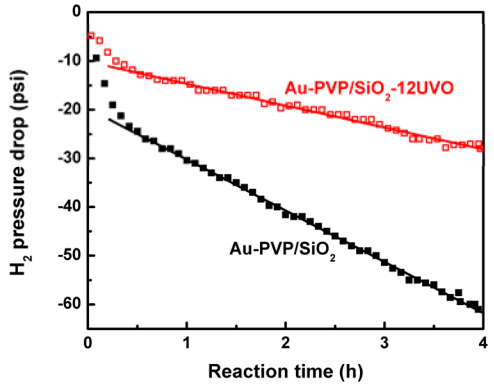

Figure 10. Hydrogen pressure drop during the catalytic hydrogenation of p-CNB over Au-PVP/SiO_2 and Au-PVP/SiO_2-12UVO catalysts.

Au-PVP/SiO_2 always led to faster pressure drops than Au-PVP/SiO_2-12UVO. The uniform pressure drops over both catalysts after ca. 0.5 h, when the reaction temperature became stabilized at 150 ± 1 °C, would mean uniform reaction rates or zero partial order in *p*-CNB because the reaction was conducted with ca. 4-fold excess of H_2, and the accumulated H_2 consumption was below ca. 15%. It would thus be reasonable to directly correlate the reaction rate constants with the $TOF_{p\text{-CNB}}$ numbers. The apparent activation energies (E_a) derived from the Arrehenius plots measured in the temperature range of 120−190 °C (Figure S5) were E_{a1} = 56.1 and E_{a2} = 45.0 kJ·mol^{-1} for Au-PVP/SiO_2 and Au-PVP/SiO_2-12UVO, respectively; their corresponding pre-exponential factors were $A_1 = 1.7 \times 10^9$ and $A_2 = 4.5 \times 10^7$ h^{-1}.

According to earlier studies,[49,50] H_2 activation would be the rate-determining step for *p*-CNB hydrogenation over oxide-supported Au NPs. Hydrogen activation by chemisorption is difficult on Au NPs or clusters,[47−49] but neutral Au NPs would be relatively more active than their negatively charged counterparts for H_2 activation by chemisorption.[5,33,46] The higher E_a for Au-PVP/SiO_2 (E_{a1}) is thus not surprising because the negatively charged Au-PVP NPs (without UVO-treatment) would become neutral when the PVP-stabilizer was eliminated by the UVO-treatment, as evidenced by the Au XPS spectra (Figure 3).

A seemingly plausible explanation for the low activity of Au-PVP/SiO_2-12UVO would thus be that the number of active sites on this catalyst was only a fraction (1/37) of that on the as-prepared Au-PVP/SiO_2 catalyst. This would hint that the

dx.doi.org/10.1021/cs501161c | ACS Catal. 2014, 4, 3982−3993

density of active sites in Au-PVP/SiO_2 was remarkably higher than that in Au-PVP/SiO_2-12UVO, which should not be the case because the Au sizes, their morphologies, and internal particle structures were essentially not changed before and after UVO-treatment (Figures 4 and 5, Table 1). We thus assume no significant difference in the number of active Au sites for Au-PVP/SiO_2 and Au-PVP/SiO_2-12UVO. The pre-exponential factors would also arise from the differences in the entropies of activation (ΔS) for the hydrogenation reaction over the two catalysts according to the transition state theory, that is $R \times \ln (A_1/A_2) = \Delta S_1 - \Delta S_2 = 30.1$ J·mol^{-1}·K^{-1}. This would point to different mobility of activated complexes in the reaction transition state on the two catalysts. A highly mobile activated complex on Au-PVP/SiO_2 could thus be assumed with the benzene ring of *p*-CNB being perpendicular to the catalytic Au surface. This orientation of the activated complex would refer to a steric function of the Au-associated PVP stabilizer in regulating the adsorption mode of the reacting CNB molecules, as depicted in Figure S6. On the other hand, the benzene ring in the activated complex on Au-PVP/SiO_2-12UVO could "lie on" or assume an orientation in parallel to the surface of the UVO-cleaned Au NPs (Figure S6), its interaction with the "open and clean" Au NPs would be significantly stronger than its perpendicularly orientated counterpart on the PVP-involving Au NPs in Au-PVP/SiO_2, and should thus have much less mobility. Thus, the higher activity of the as-prepared Au-PVP/SiO_2 catalyst would be due to that the presence of PVP could offer the reaction with a much higher entropy of activation, which compensated the energy penalty in H_2 activation.

Quantum chemical calculations showed that the adsorption energies on Au_{13} of nitrostyrene through the nitro group and of *N*-vinylpyrrolidone through the carbonyl group were 64.2 and 42.5 kJ·mol^{-1}, respectively.[51−53] Thus, the adsorption of *p*-CNB on Au NPs could be stronger than that of any single PVP monomer. But, in reality, the polymeric PVP molecules would interact with the Au NPs via more than one carbonyl groups or by multiple coordination,[5,13,43] which could lower the adsorption strength of *p*-CNB. All of these factors could contribute to the high mobility of the activated complex during the hydrogenation of *p*-CNB on the as-prepared Au-PVP/SiO_2 catalyst.

Besides the low mobility of the activated complex over the PVP-free Au-PVP/SiO_2-12UVO catalyst, the prevailing lying-on adsorption of *p*-CNB molecules at the "clean" Au NPs (Figure S6) could also result in "blockage" of some catalytically active Au sites for the reaction. This seems also consistent with the much smaller pre-exponential factor (A_2) for the reaction over this PVP-free catalyst. The activity decline of Au-PVP/SiO_2-*t*UVO at $t < 1$ h (Figure 8) would thus be mainly related to the removal of the PVP stabilizer from Au NPs since ca. 80% of the "stabilizing" PVP-residue was removed during this period (Figure 2). The very similar activity numbers by $TOF_{p\text{-CNB}}$ of all Au-PVP/SiO_2-*t*UVO at $t \geq 1$ h (including $t = 12$ h) might imply that the lying-on adsorption of *p*-CNB molecules was not sensitive to the secondary carboxylic residues. Also, it would be possible that only a small percentage of the lying-on *p*-CNB molecules could have enough reactivity, and the presence of such secondary residues could hardly change this percentage. Further discussion on effect of the secondary residues would require a complete piece of future study.

3.4.2. Modification by PVP and its Derived Residues of Au Catalysis in CAL Hydrogenation. The UVO-treatment produced a quite different impact on the catalytic performance of the Au NPs for the hydrogenation of CAL. The remarkably lower TOF_{CAL} of the as-prepared Au-PVP/SiO_2 than that of the UVO-cleaned Au-PVP/SiO_2-12UVO catalyst clearly demonstrates a negative effect of PVP stabilizer on Au catalysis for this reaction. The continuous increases in TOF_{CAL} of Au-PVP/SiO_2-*t*UVO with the UVO-treatment duration at $t > 0.5$ h further indicate that the PVP-derived carboxylic residues (secondary residues) also played negatively to the Au activity (Figure 9). These observations could be explained by envisaging a partial blockage of active Au sites by the organic residues (PVP and its derived carboxylic residues), either by direct interaction with or steric hindering of catalytic Au sites from being accessed by the reactant CAL.

However, the Au activity for CAL hydrogenation did not increase monotonously with increasing the removal degree of the organic residues. The TOF_{CAL} numbers for the samples of $t \leq 0.5$ h were even slightly lower than that for Au-PVP/SiO_2 without UVO-treatment. This would suggest that the carboxylic residues were more negative to the Au activity than PVP stabilizer; otherwise, the partial removal of PVP stabilizer by these short UVO treatments (e.g., Figures 2 and 6) would more or less enhance the Au activity. Thus, the activity changes induced by these short UVO treatments (i.e., when the removal degree of the PVP-residue was not sufficiently high) could mainly be due to that the carboxylic residues exerted a stronger electronic effect than did the original PVP stabilizer. In agreement with this explanation, the sample maximized in the carboxylic residues ($t = 0.5$ h, Figure 2) exhibited the lowest Au activity (Figure 9).

The product selectivity of CAL hydrogenation also varied remarkably on increasing the removal degree of the organic residues. The "UVO-cleaned" Au NPs (Au-PVP/SiO_2-12UVO) showed the maximum selectivity (87%) toward HCAL or the hydrogenation at the C═C bond. A significantly higher selectivity toward the hydrogenation at the C═C rather than the C═O bond seems to be an intrinsic propensity of Au NPs on noninteracting SiO_2 support because Au/SiO_2 catalysts from other preparations also showed this kind of chemoselectivity in hydrogenation of α,β-unsaturated aldehydes.[34,36,54] Previously, a UVO-treatment of PVP-stabilized Pd NPs was found effective in enhancing the catalytic activity of Pd NPs for ethylene hydrogenation.[28]

The remarkable changes in the product selectivity of CAL hydrogenation according to the removal degree of the organic residues (or UVO-treatment duration *t*) could be explained as a main consequence of the steric effect of the PVP stabilizer and its derived carboxylic residues. A preferred activation of the terminal C═O bond for the hydrogenation of CAL would become relatively unfavorable on increasing the removal degree of the residues since this C═O bond should be much less sensitive to the steric hindrance than the C═C bond. The observed continuous decline in the COL selectivity in Figure 9 is in line with this explanation. A very recent study also showed that a deposition of thiolate self-assembled monolayers on a conventional Pt/Al_2O_3 catalyst can significantly enhance the C═O hydrogenation selectivity of CAL for COL formation.[55]

From an energy perspective, low-coordinated surface Au sites (Au_{LC}) were shown to induce a high selectivity toward the C═C bond hydrogenation of α,β-unsaturated aldehydes,[34,56] probably due to their preference to the $\pi_{C=C}$ adsorption mode.[34] At the molecular level, the PVP stabilizer and its derived residues would most likely interact with these Au_{LC} sites via their carbonyl or carboxylic groups.[33,56] Extending the

dx.doi.org/10.1021/cs501161c | ACS Catal. 2014, 4, 3982−3993

UVO-treatment duration should then increase the extent of uncovering/exposing of these Au_{LC} sites, making the Au surface more suitable for selective C=C bond activation. Therefore, both the steric and electronic/energetic factors became to favor a higher selectivity toward HCAL formation when the removal degree of the organic residues was increased by extending the UVO-treatment duration.

The Au_{LC} sites are located at the corners, edges and Au(100) facets with coordination numbers (CN) of 6, 7 and 8, respectively.[37] We propose that those organic residues bound to the Au sites at the corners (CN = 6) and edges (CN = 7) were removed mainly at the early stage of the UVO-treatment (i.e., t < 1 h, Figures 2 and 6) because their removal resulted in the most pronounced changes both in the Au activity (TOF_{CAL}) and the product selectivity (Figure 9).

Removal of the organic residues would also change the overall electronic state of the Au NPs (Figure 3). The as-prepared PVP-stabilized Au NPs could be more electron-rich and could become neutral upon increasing the removal degree of the organic residues. This change would not only benefit a preferred CAL activation at the C=C bond[35] but also promote the activation of H_2,[46,48] though the present data did not allow a discrimination between the catalytic sites responsible for CAL activation from those for H_2 activation.

3.4.3. Impact of Different Stabilizers on the Hydrogenation Catalysis of Au. The catalytic consequences of the restabilization with different stabilizers of the UVO-cleaned "bare" Au NPs in Au-PVP/SiO_2-12UVO on the hydrogenation reactions of both *p*-CNB (Table 2) and CAL (Table 3) clearly demonstrate that the nature of the stabilizer also greatly impacted the hydrogenation catalysis of Au. The even higher $TOF_{p\text{-CNB}}$ and TOF_{CAL} numbers for RePVA(Au-PVP/SiO_2-12UVO) than those for the as-prepared Au-PVP/SiO_2 would be mainly due to that H_2 activation over the PVA restabilized Au NPs was easier than over the Au-PVP NPs because the PVA restabilized Au NPs would be essentially neutral but those in Au-PVP/SiO_2 negatively charged.[5,18,21,36]

The very low $TOF_{p\text{-CNB}}$ numbers of the CTAB and Citr restabilized Au NPs (ReCTAB(Au-PVP/SiO_2-12UVO) and ReCitr(Au-PVP/SiO_2-12UVO), Table 2) could be due to that these ionic stabilizers (CTAB and Citr) could not form around Au NPs dynamic and loosely adsorbed shells for regulating the orientation of *p*-CNB molecules toward the desirable adsorption state. In particular, CTAB would form via a self-assembling dense cationic CTA-layer on the Au surface[57] and impose a severe blockage to the catalytic Au sites for *p*-CNB hydrogenation. A severe blockage to catalytic Au sites for benzyl alcohol oxidation in toluene (solvent) was reported previously by a close-packed self-assembled dodecylamine layer on the Au surface.[13] On the other hand, the CTAB restabilized Au NPs not only showed a TOF_{CAL} number close to that of Au-PVP/SiO_2 but also a higher HCAL selectivity (Table 3). These results imply that the cationic CTA-layer had actually a lower steric hindrance toward the C=C bond activation than the polymeric PVP layer, which is in line with an earlier finding that CTAB was prone to occupy terrace sites[58] or Au(100) (CN = 8) and Au(111) (CN = 9) facet sites on the present Au NPs,[37] leaving most of the corner and edge sites for the hydrogenation toward the C=C bond. This suggests that the active Au sites for CAL hydrogenation were somehow different from those for *p*-CNB hydrogenation.

In order to better understand the effect of Citr stabilizer in the ReCitr(Au-PVP/SiO_2-12UVO) catalyst, the catalytic data obtained with a reference Au-Citr/SiO_2 sample, which were prepared by SiO_2-immobilization of Au-Citr NPs (4.7 ± 0.9 nm) obtained by reduction of $HAuCl_4$ with citrate as the Au-stabilizer,[21] were also included in Tables 2 and 3. The IR spectrum for this Au-Citr/SiO_2 is shown in the bottom of Figure 7B; the very weak Citr signals agree well with earlier documentations that citrate anion is a weak stabilizer for Au NPs.[6,12−15,21] The much higher $TOF_{p\text{-CNB}}$ and TOF_{CAL} numbers of Au-Citr/SiO_2 than that of ReCitr(Au-PVP/SiO_2-12UVO) could arise from the much lower Citr coverage on the Au NPs in the former sample, as evidenced in their IR spectra (Figure 7B). In the catalytic hydrogenation of CAL, these two catalysts also produced quite different product selectivity; ReCitr(Au-PVP/SiO_2-12UVO) exhibited very higher selectivity for COL and HCOL formation, even much higher than every other catalysts in this work (Table 3). These results would be explained by assuming that the Citr anions prefer to selectively occupy the Au_{LC} sites at the corners and edges as these surface sites could be more active for the hydrogenation toward the C=C bond.[34,56] The product selectivity data over Au-Citr/SiO_2 were in the middle between those over Au-PVP/SiO_2-12UVO and Au-PVP/SiO_2, in line with the low coverage of Citr. It is thus inferred that the catalytic sites for the hydrogenation toward the C=O bond of CAL would be those of lower energy (CN = 8 or 9) on exposed Au (100) or (111) facets.[37] The adsorption of excessive Citr on the UVO-cleaned "bare" Au NPs in Au-PVP/SiO_2-12UVO would result in severe blockage of the high energy Au_{LC} sites (CN = 6 and 7), thus leading to remarkably lowered selectivity for the hydrogenation toward the C=C bond. Among all the samples involving a kind of the stabilizers, Au-Ctri/SiO_2 catalyst showed the highest activity for CAL hydrogenation (TOF_{CAL}, Table 3), but its activity for *p*-CNB hydrogenation ($TOF_{p\text{-CNB}}$, Table 2) was even significantly lower than the UVO-cleaned Au-PVP/SiO_2-12UVO catalyst. This also points to that the active Au sites and mechanism for CAL hydrogenation would be different from those for *p*-CNB hydrogenation, though their exact nature remains unclear at this stage.

Finally, we discuss the similarity and differences in catalytic performance of the PVP-involving Au NPs in Au-PVP/SiO_2, RePVP(Au-PVP/SiO_2-12UVO) and Au-PVP/SiO_2-R. The Au $TOF_{p\text{-CNB}}$ numbers were essentially the same for *p*-CNB hydrogenation but TOF_{CAL} for CAL hydrogenation in the order of RePVP(Au-PVP/SiO_2-12UVO)-W > Au-PVP/SiO_2 ≥ RePVP(Au-PVP/SiO_2-12UVO) ≈ Au-PVP/SiO_2-R1 ≈ Au-PVP/SiO_2-R4, showing that the latter reaction was more sensitive to the amount and subtle state of the polymeric PVP stabilizer. This sensitivity of CAL hydrogenation was further featured by the product selectivity data. The higher selectivity for HCAL of the extensively washed RePVP(Au-PVP/SiO_2-12UVO)-W could be due to that in addition to the elimination of ca. 20% PVP the extensive washing of the RePVP(Au-PVP/SiO_2-12UVO) would also make the "re-adsorbed" PVP-stabilizer looser or more flexible, which led to less hindrance to the reactant CAL molecules and improved the relative competitiveness of the C=C activation. On the other hand, the product selectivity data over the two Au-PVP/SiO_2-R samples were very similar to those over the as-prepared Au-PVP/SiO_2 though the amount of residual PVP in both Au-PVP/SiO_2-R was ca. 25−30% lower (Figure S4). This would be expected because the reflux treatment mainly removed those PVP molecules adsorbed on the surface of SiO_2 (support).

dx.doi.org/10.1021/cs501161c | ACS Catal. 2014, 4, 3982−3993

4. CONCLUSIONS

This work demonstrates that UVO-treatment in flowing air of PVP-stabilized Au NPs can lead to controllable removal of the stabilizer and its derived residues according to the UVO-treatment duration without impacting the size and morphology of the Au NPs. Photochemical oxidation of the PVP-stabilizer to surface intermediates involving carboxylic groups was disclosed by FTIR and XPS measurements of the samples with various UVO-treatment durations. Au NPs completely free of the residues have been obtained by extending the treatment for 12 h. This technique of UVO-treatment has proven advantageous to the washing method by refluxing in water.

On variation of the removal degree of PVP and it derived residues, it is clearly shown that the presence of residual PVP stabilizer was quite beneficial to the Au activity for *p*-CNB hydrogenation but was detrimental to the activity for CAL hydrogenation. Rich information on the product selectivity changes has been gained in the catalytic CAL hydrogenation, which shows some subtle effects of the residues on the hydrogenation catalysis of nanosized Au. These effects of PVP stabilizer on the hydrogenation catalysis of Au are further confirmed by "restabilization" with PVP of the UVO-treated Au NPs. The "restabilization" with different stabilizer molecules (PVP, PVA, CTAB and Citr) of the UVO-cleaned Au NPs has made it possible to prepare for the first time the same Au NPs involving stabilizers of different nature, the use of which for the catalytic studies has enabled a comprehension of stabilizer impact on the hydrogenation catalysis of Au NPs.

■ ASSOCIATED CONTENT

Supporting Information

Assignments of infrared absorptions associated with PVP-stabilizer in the as-prepared Au-PVP/SiO_2, elemental composition and molar ratios of N/Au, N/Si and $C^{\delta+}/C^0$ determined by XPS for Au-PVP/SiO_2 samples of different UVO-treatment durations, experimental setup for the UVO-treatment, Madon–Boudart tests for the catalytic hydrogenation of CAL and *p*-CNB on Au-PVP/SiO_2 catalysts of varying Au loadings, FTIR spectra for PVP-SiO_2 samples (no Au NPs) of different UVO-treatment durations, IR spectra of Au-PVP/SiO_2-R1, Au-PVP/SiO_2-R4 and Au-PVP/SiO_2, Arrhenius plots for the hydrogenation reaction of *p*-CNB over Au-PVP/SiO_2 and Au-PVP/SiO_2-12UVO, adsorption and activation of *p*-CNB and H_2 on Au NPs with and without the PVP-stabilizer. This material is available free of charge via the Internet at http://pubs.acs.org.

■ AUTHOR INFORMATION

Corresponding Author

*E-mail: bqxu@mail.tsinghua.edu.cn.

Notes

The authors declare no competing financial interest.

■ ACKNOWLEDGMENTS

Financial supports from national Natural Science Foundation of China (grant nos. 21033004 and 21221062), National Basic Research Program of China (2013CB933103) and Tsinghua University (20131089311) are acknowledged.

■ REFERENCES

(1) Haruta, M. *Catal. Today* **1997**, *36*, 153–166.
(2) Tsunoyama, H.; Sakurai, H.; Tsukuda, T. *Chem. Phys. Lett.* **2006**, *429*, 528–532.
(3) Prati, L.; Martra, G. *Gold Bull.* **1999**, *32*, 96–101.
(4) Yu, Y.; Zhang, Q.-B.; Xie, J.-P.; Lu, X.-M.; Lee, J. Y. *Nanoscale* **2011**, *3*, 1497–1500.
(5) Zhang, G.-R.; Xu, B.-Q. *Nanoscale* **2010**, *2*, 2798–2804.
(6) Xia, X.-H.; Yang, M.-X.; Wang, Y.-C.; Zheng, Y.-Q.; Li, Q.-G.; Chen, J.-Y.; Xia, Y.-N. *ACS Nano* **2012**, *6*, 512–522.
(7) Mertens, P. G. N.; Poelman, H.; Ye, X.; Vankelecom, I. F. J.; Jacobs, P. A.; De Vos, D. E. *Catal. Today* **2007**, *122*, 352–360.
(8) Kristian, N.; Yan, Y.; Wang, X. *Chem. Commun.* **2008**, *3*, 353–355.
(9) Yang, X.-W.; Zhang, G.-R.; Li, Y.-X.; Xu, B.-Q. *Acta Phys. -Chim. Sin.* **2009**, *25*, 2565–2569.
(10) Sun, K.-Q.; Hong, Y.-C.; Zhang, G.-R.; Xu, B.-Q. *ACS Catal.* **2011**, *1*, 1336–1346.
(11) Zhao, B.; Chen, Y.-W. *Mater. Chem. Phys.* **2011**, *125*, 763–768.
(12) Porta, F.; Prati, L.; Rossi, M.; Coluccia, S.; Martra, G. *Catal. Today* **2000**, *61*, 165–172.
(13) Quintanilla, A.; Butselaar-Orthlieb, V. C. L.; Kwakernaak, C.; Sloof, W. G.; Kreutzer, M. T.; Kapteijn, F. *J. Catal.* **2010**, *271*, 104–114.
(14) Grunwaldt, J.-D.; Kiener, C.; Wogerbauer, C.; Baiker, A. *J. Catal.* **1999**, *181*, 223–232.
(15) Tsubota, S.; Nakamura, T.; Tanaka, K.; Haruta, M. *Catal. Lett.* **1998**, *56*, 131–135.
(16) Lopez-Sanchez, J. A.; Dimitratos, N.; Hammond, C.; Brett, G. L.; Kesavan, L.; White, S.; Miedziak, P.; Tiruvalam, R.; Jenkins, R. L.; Carley, A. F.; Knight, D.; Kiely, C. J.; Hutchings, G. J. *Nat. Chem.* **2011**, *3*, 551–556.
(17) Yin, H.-Y.; Ma, Z.; Chi, M.-F.; Dai, S. *Catal. Lett.* **2010**, *136*, 209–221.
(18) Tsunoyama, H.; Ichikuni, N.; Sakurai, H.; Tsukuda, T. *J. Am. Chem. Soc.* **2009**, *131*, 7086–7093.
(19) Villa, A.; Wang, D.; Su, D.-S.; Prati, L. *ChemCatChem* **2009**, *1*, 510–514.
(20) Lee, K. Y.; Lee, Y. W.; Lee, J.-H.; Han, S. W. *Colloids Surf., A* **2010**, *372*, 146–150.
(21) Zhong, R.; Yan, X.; Gao, Z.; Zhang, R.; Xu, B. *Catal. Sci. Technol.* **2013**, *3*, 3013–3019.
(22) Moran, C. H.; Rycenga, M.; Zhang, Q.; Xia, Y.-N. *J. Phys. Chem. C* **2011**, *115*, 21852–21857.
(23) Ansar, S. M.; Ameer, F. S.; Hu, W.; Zou, S.; Charles, U. P.; Zhang, D. *Nano Lett.* **2013**, *13*, 1226–1229.
(24) Hui, C.-L.; Li, X.-G.; Hsing, I.-M. *Electrochim. Acta* **2005**, *51*, 711–719.
(25) Kuhn, J. N.; Tsung, C.-K.; Huang, W.; Somorjai, G. A. *J. Catal.* **2009**, *265*, 209–215.
(26) Vig, J. R. *J. Vac. Sci. Technol. A* **1985**, *3*, 1027–1034.
(27) Aliaga, C.; Park, J. Y.; Yamada, Y.; Lee, H.-S.; Tsung, C.-K.; Yang, P.-D.; Somorjai, G. A. *J. Phys. Chem. C* **2009**, *113*, 6150–6155.
(28) Crespo-Quesada, M.; Andanson, J.-M.; Yarulin, A.; Lim, B.; Xia, Y.-N.; Kiwi-Minsker, L. *Langmuir* **2011**, *27*, 7909–7916.
(29) Guczi, L.; Peto, G.; Beck, A.; Frey, K.; Geszti, O.; Molnar, G.; Daroczi, C. *J. Am. Chem. Soc.* **2003**, *125*, 4332–4337.
(30) He, D.-P.; Shi, H.; Wu, Y.; Xu, B.-Q. *Green Chem.* **2007**, *9*, 849–851.
(31) Corma, A.; Serna, P. *Science* **2006**, *313*, 332–334.
(32) Chen, Y.-Y.; Qiu, J.-S.; Wang, X.-K.; Xiu, J.-H. *J. Catal.* **2006**, *242*, 227–230.
(33) Claus, P. *Appl. Catal., A* **2005**, *291*, 222–229.
(34) Yang, X.-F.; Wang, A.-Q.; Wang, X.-D.; Zhang, T.; Han, K.-L.; Li, J. *J. Phys. Chem. C* **2009**, *113*, 20918–20926.
(35) Milone, C.; Ingoglia, R.; Schipilliti, L.; Crisafulli, C.; Neri, G.; Galvagno, S. *J. Catal.* **2005**, *236*, 80–90.
(36) Shi, H.; Xu, N.; Zhao, D.; Xu, B.-Q. *Catal. Commun.* **2008**, *9*, 1949–1954.
(37) Zhang, G.-R.; Zhao, D.; Feng, Y.-Y.; Zhang, B.-S.; Su, D.-S.; Liu, G.; Xu, B.-Q. *ACS Nano* **2012**, *6*, 2226–2236.
(38) Singh, U. K.; Vannice, M. A. *Appl. Catal., A* **2001**, *213*, 1–24.

(39) Borodko, Y.; Habas, S. E.; Koebel, M.; Yang, P.-D.; Frei, H.; Somorjai, G. A. *J. Phys. Chem. B* **2006**, *110*, 23052−23059.
(40) Uosaki, K.; Emran Quayum, M.; Nihonyanagi, S.; Kondo, T. *Langmuir* **2004**, *20*, 1207−1212.
(41) Innocenzi, P. *J. Non-Cryst. Solids* **2003**, *316*, 309−319.
(42) Ndiege, N.; Chandrasekharan, R.; Radadia, A. D.; Harris, W.; Mintz, E.; Masel, R. I.; Shannon, M. A. *Chem.—Eur. J.* **2011**, *17*, 7685−7693.
(43) Jiang, P.; Zhou, J.-J.; Li, R.; Wang, Z.-L.; Xie, S.-S. *Nanotechnology* **2006**, *17*, 3533−3538.
(44) Prause, S.; Spange, S. *J. Phys. Chem. B* **2004**, *108*, 5734−5741.
(45) Lai, Y. J. *Appl. Polym. Sci.* **1997**, *66*, 1475−1484.
(46) Kang, G.-J.; Chen, Z.-X.; Li, Z.; He, X. *J. Chem. Phys.* **2009**, *130*, 0347013.
(47) Bus, E.; Miller, J. T.; van Bokhoven, J. A. *J. Phys. Chem. B* **2005**, *109*, 14581−14587.
(48) Corma, A.; Boronat, M.; Gonzalez, S.; Illas, F. *Chem. Commun.* **2007**, *43*, 3371−3373.
(49) Serna, P.; Concepcion, P.; Corma, A. *J. Catal.* **2009**, *265*, 19−25.
(50) He, D.-P.; Jiao, X.-D.; Jiang, P.; Wang, J.; Xu, B.-Q. *Green Chem.* **2012**, *14*, 111−116.
(51) Boronat, M.; Concepcion, P.; Corma, A.; Gonzalez, S.; Illas, F.; Serna, P. *J. Am. Chem. Soc.* **2007**, *129*, 16230−16237.
(52) Peniche, C.; Zaldivar, D.; Pazos, M.; Paz, S.; Bulay, A.; Roman, J. *J. Appl. Polym. Sci.* **1993**, *50*, 485−493.
(53) Okumura, M.; Kitagawa, Y.; Kawakami, T.; Haruta, M. *Chem. Phys. Lett.* **2008**, *459*, 133−136.
(54) Bailie, E. J.; Hutchings, G. J. *Chem. Commun.* **1999**, *21*, 2151−2152.
(55) Kahsar, K. R.; Schwartz, D. K.; Medlin, J. W. *J. Am. Chem. Soc.* **2014**, *136*, 520−526.
(56) Mohr, C.; Hofmeister, H.; Claus, P. *J. Catal.* **2003**, *213*, 86−94.
(57) Gole, A.; Murphy, C. J. *Chem. Mater.* **2005**, *17*, 1325−1330.
(58) Hernandez, J.; Solla-Gullon, J.; Herrero, E.; Aldaz, A.; Feliu, J. M. *J. Phys. Chem. C* **2007**, *111*, 14078−14083.